Cancer Immunology, Immunotherapy (2025) 74:240
https://doi.org/10.1007/s00262-025-04074-4

RESEARCH

# Glutamate transporter SLC1A6 promotes resistance to immunotherapy in cancer

**Chenchen Li[1] · Yi Lin[2,3] · Haoran Zheng[2,3] · Hengda Zeng[4] · Longhao Xu[2,3] · Daqin Wu[2,3] · Jianwen Lao[2,3] · Peicong Cai[2,3] · Shuai Liang[2,3] · Chunhui Wang[5] · Tianxin Lin[2,3,4] · Wenlong Zhong[2,3]**

Received: 5 March 2025 / Accepted: 30 April 2025


## Abstract

**Background** Resistance to immune checkpoint inhibitors remains a significant challenge in the treatment of cancer. Emerging evidence suggests that metabolic reprogramming plays a crucial role in tumor metabolism and progression. Our study strived to investigate the role and underlying mechanisms of the glutamate transporter SLC1A6 in resistance to immunotherapy of cancer.

**Methods** Single-cell RNA sequencing was performed on bladder cancer patients receiving neoadjuvant immunotherapy to identify the expression of SLC1A6 in treatment-resistant cases. The clinical prognostic value of SLC1A6 in cancer was validated using publicly available lung cancer single-cell datasets, as well as transcriptomic data from both bladder and lung cancer cohorts. Flow cytometry was employed to assess the impact of SLC1A6 knockdown on the effector function of $CD8^+$ T cell. In vivo tumor models were used to evaluate the role of SLC1A6 in immunotherapy resistance, with immunofluorescence staining performed to examine $GZMB^+$ $CD8^+$ T cell infiltration.

**Results** SLC1A6 was highly expressed in bladder cancer patients resistant to neoadjuvant immunotherapy, and its expression was associated with disease progression, poor prognosis, and low immune infiltration. Knockdown of SLC1A6 in tumor cells enhanced $CD8^+$ T cell effector function. SLC1A6 knockdown also improved the efficacy of immunotherapy and increased the infiltration of $GZMB^+$ $CD8^+$ T cells within the tumor microenvironment.

**Conclusions** SLC1A6 plays a critical role in resistance to immunotherapy in cancer. Targeting SLC1A6 may provide a promising therapeutic strategy for improving responses to neoadjuvant immunotherapy and advancing combination treatment approaches.

**Keywords** Cancer treatment · SLC1A6 · Immunotherapy · T cells

## Introduction

In recent years, immune checkpoint inhibitors (ICIs), particularly PD-L1/PD-1 inhibitors, have revolutionized cancer treatment, showing significant clinical benefits, especially in

Chenchen Li, Yi Lin, Haoran Zheng and Hengda Zeng have contributed equally to this work.

✉ Tianxin Lin
lintx@mail.sysu.edu.cn

✉ Wenlong Zhong
zhongwlong3@mail.sysu.edu.cn

[1] Department of Medical Oncology, The Sixth Affiliated Hospital, Sun Yat-Sen University, Guangzhou, People's Republic of China

[2] Department of Urology, Sun Yat-Sen Memorial Hospital, Sun Yat-Sen University, Guangzhou, People's Republic of China

[3] Guangdong Provincial Key Laboratory of Malignant Tumor Epigenetics and Gene Regulation, Sun Yat-Sen Memorial Hospital, Sun Yat-Sen University, Guangzhou, People's Republic of China

[4] Department of Urology, The Fifth Affiliated Hospital of Sun Yat-Sen University, Zhuhai, Guangdong, People's Republic of China

[5] Department of Urology, Yan'an Hospital Affiliated With Kunming Medical University, Kunming, People's Republic of China

Published online: 07 June 2025

patients with metastatic disease [1–3]. The efficacy of these therapies is primarily attributed to the high immunogenicity of cancer, characterized by elevated PD-L1 expression and a high tumor mutation burden (TMB) [4]. Increasing evidence underscores the pivotal role of immune regulation in cancer initiation and progression, with the immune system maintaining a dynamic balance between tumor-promoting and tumor-suppressing responses [5]. Consequently, immune-based therapeutic strategies have gained considerable attention in cancer diagnosis and treatment [6]. Recent advances in cancer immunology have provided critical insights into the complex immune landscape of various malignancies, elucidating the roles of immune cell populations and immune effector molecules within the tumor microenvironment (TME), which are closely associated with clinical outcomes [7, 8]. However, despite these advancements, a substantial proportion of patients show unresponsive to current immunotherapeutic approaches with limited subsequent treatment options [9, 10]. The heterogeneity of the TME among individuals contributes to variability in responses to immune checkpoint blockade, highlighting the urgent need to uncover the mechanisms underlying immunotherapy resistance and develop novel precision medicine strategies for cancer [11, 12].

SLC1A6 (Solute Carrier Family 1 Member 6) is a sodium-dependent glutamate transporter primarily involved in neuronal function, neuroprotection, and maintaining glutamate homeostasis [13–15]. Emerging evidence suggests that SLC1A6 also plays a crucial role in tumor metabolism and progression [16–18]. To sustain rapid proliferation, tumor cells often undergo metabolic reprogramming, with glutamate acting as a key metabolic intermediate essential for tumor growth and survival [19]. According to previous studies, glutamate metabolism plays a central role in tumor progression by fueling glutaminolysis, supporting the tricarboxylic acid (TCA) cycle, and maintaining redox balance through glutathione biosynthesis, further influencing tumor cell plasticity and immune evasion [20–22]. By modulating SLC1A6 expression or function, tumor cells can alter glutamate uptake and metabolism, thereby facilitating tumor progression, enhancing therapeutic resistance, and promoting metabolic reprogramming and immune evasion. Thus, in addition to its well-established role in the nervous system, SLC1A6-mediated metabolic regulation in tumor cells represents a potential therapeutic target.

In this study, we identified SLC1A6 as a key driver of immunotherapy resistance in bladder cancer using single-cell RNA sequencing analysis. Its clinical relevance was further supported by analyses of publicly available lung cancer single-cell datasets, as well as transcriptomic data from both bladder and lung cancer cohorts. Functional assays conducted in vitro and in vivo provided additional evidence supporting its role in immune evasion and therapeutic resistance. Our findings suggest that targeting SLC1A6 may represent a promising strategy for improving the efficacy of neoadjuvant immunotherapy in cancer.

## Methods

### Single-cell RNA sequencing and data processing

Lung cancer single-cell RNA sequencing data were obtained from the Gene Expression Omnibus (GEO) repository under accession number GSE189357. Raw single-cell RNA sequencing data of bladder cancer samples were aligned with the GRCh38 human reference genome and processed using the Cell Ranger (v3.0, 10×Genomics). Unique molecular identifier (UMI) counts were quantified, and a gene-cell barcode matrix was generated for downstream analysis, which was then converted into a Seurat object using the Seurat R package (v5.1.0). Low-quality cells were filtered out based on the following criteria: (i) fewer than 200 detected genes, (ii) more than 6000 detected genes, and (iii) mitochondrial UMI counts exceeding 20%. Genes detected in fewer than three cells were also removed. After quality control, the UMI count matrix was log-normalized and scaled. Principal component analysis (PCA) was performed using the top 3000 variable genes. Harmony (v1.2.3) was applied to mitigate potential batch effects. Then, cell clusters were identified using the FindClusters function with a resolution of 0.5 and visualized using uniform manifold approximation and projection (UMAP) plots. Cluster-specific differentially expressed genes were identified using the FindAllMarkers function and used for cell type annotation. Tumor cells were then subset and reclustered for further analysis.

### Transcriptomic data analysis

Transcriptomic sequencing was performed on 47 bladder cancer patients from Sun Yat-sen Memorial Hospital (SYSMH). The TCGA datasets of bladder cancer and lung cancer were downloaded from "https://www.cancer.gov/ccg/research/genome-sequencing/tcga". The optimal cutoff for SLC1A6-based survival grouping was determined using the surv_cutpoint function from the survminer R package (v0.4.9). Kaplan–Meier survival curves were generated, and log-rank tests were used to assess statistical significance. Immune infiltration analysis was performed using the CIBERSORT (v0.1.0), ESTIMATE (v1.0.13), and GSVA (v1.46.0) R packages.

### Gene set enrichment analysis (GSEA)

GSEA was performed using the clusterProfiler R package (v4.12.6). The ranked gene list was generated based on log2

fold-change values obtained from differential expression analysis using the DESeq2 package (v1.44.0). The reference gene sets were downloaded from "https://www.gsea-msigdb.org/gsea/msigdb".

## Cell lines and cell culture

HEK293T cell line (RRID: CVCL_0063) and murine Lewis lung carcinoma cell line LLC (RRID: CVCL_4358) were obtained from the American Type Culture Collection (ATCC), and the murine bladder cancer cell line MB49 (RRID: CVCL_7076) was obtained from Millipore. HEK293T cells, LLC cells, and MB49 cells were cultured in Dulbecco's modified Eagle's medium (DMEM), contained 10% fetal bovine serum (FBS), 100 U/ml penicillin, and 100 µg/ml streptomycin (HyClone, Thermo, USA). All cells were cultured in a humidified atmosphere of 5% $CO_2$ at 37 °C. All cell lines used in this study were tested for mycoplasma contamination and found to be negative.

For in vitro experiments, exogenous glutamate (MCE, HY-14608) was added to the culture system at a concentration of 1 mM.

## Lentivirus preparation and transduction

The forward sequence of the shRNA targeting SLC1A6 is CCGGCGGCATCCTAATGGTTACCATCTCGAGATGGTAACCATTAGGATGCCGTTTTTG, and the reverse sequence is AATTCAAAAACGGCATCCTAATGGTTACCATCTCGAGATGGTAACCATTAGGATGCCG. shRNA sequence targeting SLC1A6 was encoded in pLKO.1-puro lentiviral vectors. For lentiviral production, HEK293T cells were co-transfected with the pLKO.1-shRNA plasmid, the packaging plasmid psPAX2, and the envelope plasmid pMD2.G at a ratio of 4:3:1, using polyethyleneimine (PEI) reagent (Sigma-Aldrich) according to the manufacturer's protocol. After 48 h post-transfection, lentiviral supernatants were collected, filtered through a 0.45-µm membrane, and concentrated using ultracentrifugation.

For lentiviral transduction, MB49 cells or LLC cells were seeded at a density of $5\times10^5$ cells per well in a 6-well plate, and transduced with lentiviral supernatants in the presence of 8 µg/mL polybrene. After 48 h of incubation, the culture medium was replaced with fresh complete DMEM to remove residual viral particles. Transduction efficiency was validated by qRT-PCR and western blot to confirm SLC1A6 knockdown.

## Isolation and culture of primary mouse T cells

Primary mouse T cells were harvested from the spleens of C57BL/6 mice under sterile conditions. Single-cell suspensions were prepared by gently pressing the organs through a 70-µm mesh filter. Red blood cells were lysed using RBC lysis buffer. T cells were isolated using a CD3 T cell isolation kit (BioLegend) following the manufacturer's protocol. Briefly, the cell suspension was incubated with biotin antibody cocktail specific for non-$CD3^+$ cell markers, followed by incubation with magnetic beads coated with anti-biotin antibodies. $CD3^+$ T cells were then separated using a magnetic column and eluted.

Isolated $CD3^+$ T cells were eluted from the column and resuspended in complete RPMI-1640 medium (containing 10% FBS, 100 U/mL penicillin, 100 µg/mL streptomycin, 100 U/ml mouse recombinant IL-2) and plated in 24-well or 6-well plates. The cells were activated by adding 1 µg/mL anti-CD3 (Biogems Cat# 05112-25, RRID: AB_3099697) and 1 µg/mL anti-CD28 (Biogems Cat# 10312-25, RRID: AB_3099698). The cells were cultured in a humidified incubator at 37 °C with 5% $CO_2$. After 3–4 days, the cells were harvested for downstream analyses.

## qRT-PCR

RNA was extracted from cells by TRIzol reagent (Thermo Fisher Scientific). RNA concentration and quality were assessed using a NanoDrop 2000 (Thermo Fisher Scientific). RNA was reverse-transcribed with HiScript III RT SuperMix (Vazyme), and ChamQ Universal SYBR qPCR Master Mix (Vazyme) was used to amplify cDNA according to the manufacturer's standard protocol. LightCycler 480 real-time instrument (Roche, Germany) was applied to perform the real-time qPCR. Relative gene expression levels were determined using the $2^{-\Delta\Delta Ct}$ method after normalizing to β-actin levels. All primer sequences are provided in Table 1.

## Western blotting

Lysates of cells were prepared in RIPA buffer (CW2333S, CWBio) supplemented with protease and phosphatase inhibitors. Protein concentration was measured by BCA Protein Assay (Thermo Fisher, 23227). Then, proteins were resolved by SDS-PAGE after adding loading buffer and transferred onto polyvinylidene difluoride (PVDF) membranes. The PVDF membranes were blocked with 5% skimmed milk for

**Table 1** Primer sequences for qRT-PCR

| Gene | Forward (5′–3′) | Reverse (5′–3′) |
|---|---|---|
| β-Actin | CATTGCTGACAGGATGCAGAAGG | TGCTGGAAGGTGGACAGTGAGG |
| Slc1a6 | AGCAGCCACGGCAATAGTC | ATGCCAAGCTGACACCAATGA |

1 h at room temperature and incubated with the corresponding primary antibodies at 4 °C overnight. The primary antibodies used for western blot consisted of anti-SLC1A6 (1:2000, Proteintech Cat# 12876-1-AP, RRID: AB_10642147) and anti-GAPDH (1:50,000, Proteintech Cat# 60004-1-Ig, RRID: AB_2107436). The next day, PVDF membranes were incubated with secondary antibodies, and protein signals were visualized using the UltraSignal ECL reagent (4AW011, 4A Biotech) to determine expression levels.

## Flow cytometry

Cells were harvested and washed with ice-cold PBS. For surface staining, cells were incubated with fluorophore-conjugated antibodies targeting specific surface markers for 30 min at 4 °C protected from light. For intracellular staining, the Foxp3/Transcription Factor Staining Buffer Set (Thermo Fisher Scientific) was used for fixation and permeabilization. After permeabilization, cells were stained with antibodies targeting intracellular targets for 30 min at 4 °C. The following antibodies were used: anti-CD8a APC (BioLegend Cat# 162305, RRID: AB_2927947) and anti-GZMB FITC (BioLegend Cat# 515403, RRID: AB_2114575). Prior to acquisition, samples were filtered through a 40-μm cell strainer to ensure a single-cell suspension. Data were acquired and analyzed on CytoFLEX (Beckman Coulter).

## CCK8 assay

Cell proliferation was assessed using the CCK8 assay (Biosharp). MB49 cells or LLC cells were seeded into 96-well plates at $5 \times 10^3$ cells per well and incubated overnight. Cells were then treated with different conditions. After incubation, 10 μL of CCK8 solution was added to each well at different time points, and cells were further incubated for an additional 2 h. Absorbance was measured at 450 nm using a microplate reader.

## Transwell migration assay

For migration assays, MB49 cells or LLC cells were suspended in 200 μL serum-free medium and seeded in the upper chambers (8-μm pore, Corning). A total 700 μL medium with 10% FBS was added into the lower chambers. After incubation for 24 h with 5% CO2 at 37 °C, the cells in the upper chamber were removed. Then, the cell culture inserts were gently washed by PBS and invaded cells on the lower surface were fixed by 4% paraformaldehyde. Finally, the cells were stained with crystal violet for photographing and counting.

## Detection of glutamate

Glutamate levels were quantified using a Glutamic acid ELISA Kit (CB10320-Mu) according to the manufacturer's protocol. Briefly, 50 μL of cell lysates, supernatants, or standard solutions, along with 100 μL of HRP-conjugate reagent, were added to pre-coated 96-well plates and incubated for 1 h at 37 °C. After washing, chromogen solution was added and incubated for 15 min at 37 °C. The reaction was stopped with 50 μL of stop solution, and the absorbance was measured at 450 nm. Glutamate levels were determined by comparing the OD values of samples with the standard curve.

## Animals

Female C57BL/6 mice (4–5 weeks old) were maintained in a specific pathogen-free (SPF) barrier facility at the Laboratory Animal Center, Guangzhou LingFu TopBiotech. Co., LTD (Guangzhou, China). MB49 or LLC cells were trypsinized, counted, and subcutaneously injected into the dorsal flank of each mouse ($5 \times 10^5$ cells per mouse) to establish a tumor model. Starting on day 3, mice received intraperitoneal injections of 200 μg PD-1 blocking antibody (Bio X Cell Cat# BE0146, RRID: AB_10949053) or 200 μg PD-L1 blocking antibody (Bio X Cell Cat# BE0101, RRID: AB_10949073) every three days for a total of six doses, and an equal dose of isotype antibody (Bio X Cell Cat# BE0089, RRID: AB_1107769) was used for control. Tumor growth was monitored every three days using a caliper, and tumor volume was calculated as $0.5 \times L \times W^2$, where L represents tumor length and W represents tumor width. Mice were killed on day 21, and tumor tissues were harvested and weighed for subsequent analysis.

## Immunofluorescence staining

All tissue sections were deparaffinized in xylene and rehydrated through a graded series of ethanol. Antigen retrieval was conducted using citrate buffer (pH 6.0) in a pressure cooker for 20 min. To minimize nonspecific binding, the sections were blocked with 5% BSA for 30 min at room temperature. Primary antibodies diluted in blocking solution were incubated with the sections overnight at 4 °C in a humidified chamber. The tissues were then incubated with fluorochrome-conjugated secondary antibodies for 1 h at room temperature protected from light. Subsequentially, DAPI was used for counterstaining the nuclei. Automated Quantitative Pathology Imaging System (Akoya Vectra Polaris) was used to obtain the images. Three random fields of view per section were analyzed. The primary antibodies used for immunofluorescence staining consisted of anti-CD8α (1:2000, Cell Signaling Technology Cat#

98941, RRID: AB_2756376), anti-GZMB (1:1000, Cell Signaling Technology Cat# 44153, RRID: AB_2857976).

### Statistical analysis

All statistical graphs and corresponding statistical analyses were performed using GraphPad Prism 9 software, and error bars indicate S.E.M. or S.D., unless otherwise indicated. The statistical significance of differences between groups was determined by unpaired Student's t test, one-way ANOVA, or two-way ANOVA. All other statistical analyses in the present study were performed using R (version 4.4.0). Calculated $P$ values were given by number and asterisk(s). *$P<0.05$; **$P<0.01$; ***$P<0.001$; ****$P<0.0001$.

## Results

### Single-cell RNA sequencing analysis of neoadjuvant immunotherapy in bladder cancer patients

To investigate the factors associated with resistance to neoadjuvant immunotherapy in bladder cancer, we performed single-cell RNA sequencing analysis on eight bladder cancer patients who underwent neoadjuvant immunotherapy, including four immunotherapy-sensitive cases and four immunotherapy-resistant cases (Fig. 1A). Following strict quality control measures and standard single-cell analysis workflows, including batch effect correction and dimensionality reduction, unsupervised clustering identified 20 cell clusters in total (Fig. S1A). These clusters were classified into eight major cell types based on canonical markers:

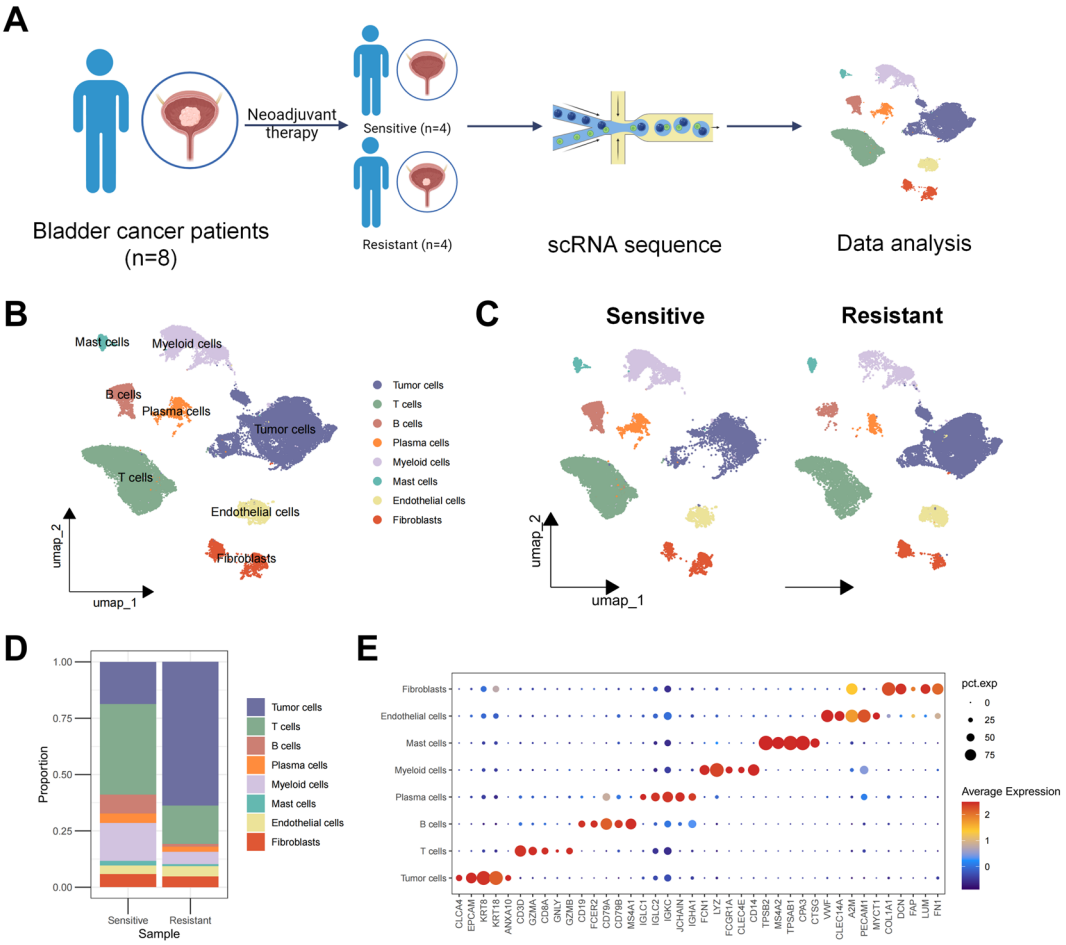


**Fig. 1** Single-cell transcriptomic profiling of neoadjuvant immunotherapy response in bladder cancer. **A** Overview of the study design and flowchart of the single-cell RNA sequencing analysis of eight bladder cancer samples (therapy-sensitive, $n=4$; therapy-resistant, $n=4$). **B** Uniform Manifold Approximation and Projection (UMAP) plot displaying the major cell types from all samples. Each dot represents an individual cell, with eight distinct colors indicating different cell populations. **C** UMAP plot of patient grouping based on the outcome of neoadjuvant therapy. **D** Stacked bar plot illustrating the proportions of major cell types in the sensitive and resistant groups. **E** Bubble plot depicting the expression of marker genes for each major cell type

epithelial cells (tumor cells) (EPCAM), T cells (CD3D, GZMB), B cells (CD79A, MS4A1), plasma cells (JCHAIN), myeloid cells (LYZ, CD68), mast cells (TPSAB1), fibroblasts (FAP, COL1A1), and endothelial cells (VWF) (Fig. 1B). Notably, the majority of the cellular population in immunotherapy-resistant patients consisted of tumor cells, while T cell subsets demonstrated reduced proportions in the neoadjuvant immunotherapy-resistant group (Fig. S1B, Fig. 1C, D). The key marker molecules used to annotate the cell subpopulations are depicted in Fig. 1E and Fig S1C.

## SLC1A6 is associated with immunotherapy resistance in bladder cancer

To further identify key molecules related to neoadjuvant immunotherapy resistance in bladder cancer, we performed reclustering of epithelial cells, which revealed seven distinct tumor subclusters (Fig. 2A). A comparative analysis of the subcluster composition between the treatment-resistant and treatment-sensitive groups showed specific enrichment of the tumor_c7 subcluster in the resistant group (Fig. 2B). The key marker genes defining each tumor subcluster are presented in Fig. 2C and Figure S2A.

Subsequently, we conducted differential expression analysis of tumor cells between the sensitive and resistant groups. Among the top upregulated genes in the resistant group, SLC1A6 was identified (Fig. S2B). Notably, SLC1A6 was specifically expressed in the tumor_c7 subcluster, which was specifically enriched in the immunotherapy-resistant group (Fig. 2D, Fig. S2C). Gene Set Enrichment Analysis (GSEA) of differentially expressed genes in the tumor_c7 subcluster revealed the downregulation of immune activation pathways compared to other clusters (Fig. 2E). Collectively, these findings suggest that SLC1A6 is associated with neoadjuvant immunotherapy resistance in bladder cancer.

Furthermore, we validated our findings in lung cancer dataset. Applying the consistent analytical pipeline, tumor cells were extracted and reclustered into four malignant subclusters, with subcluster c3_tumor demonstrating exclusive upregulation of SLC1A6 (Fig. S3A-B). GSEA revealed negative correlation between c3_tumor and immune-related pathways, recapitulating our observations in bladder cancer (Fig. S3C).

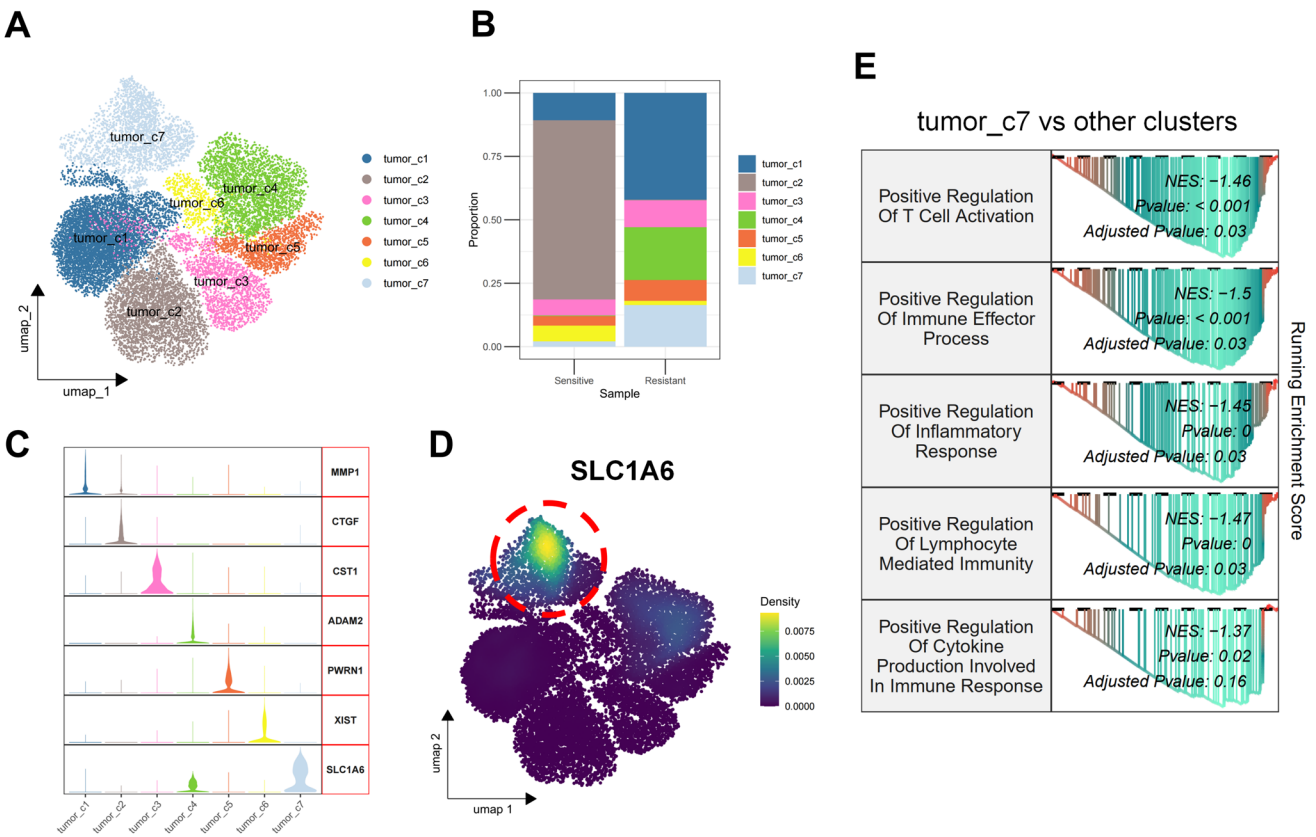


**Fig. 2** SLC1A6 is associated with immunotherapy resistance in bladder cancer. **A** UMAP plot depicting tumor cell subclusters after reclustering. **B** Stacked bar plot illustrating the proportions of tumor cell subclusters in the sensitive and resistant groups. **C** Violin plot showing marker genes for each tumor cell subcluster after reclustering. **D** UMAP density plot illustrating the expression of SLC1A6. **E** GSEA results illustrating the enriched pathways between the tumor_c7 subcluster and other tumor subclusters

## Correlation of SLC1A6 expression with bladder cancer progression and immune infiltration

To further evaluate the clinical significance of SLC1A6 in bladder cancer, we collected and analyzed data from TCGA database. Our findings revealed that SLC1A6 expression was significantly higher in tumor tissues than in normal tissues (Fig. 3A). Additionally, we compared SLC1A6 expression levels across different pathological T and N stages in bladder cancer patients and observed a positive correlation between SLC1A6 expression and advanced pathological T and N stages, with higher expression levels associated with disease progression (Fig. 3B, C). Next, we stratified bladder cancer patients into SLC1A6-low and SLC1A6-high expression groups based on expression levels. Survival analysis showed that patients in the SLC1A6-low group had a better prognosis than those in the SLC1A6-high group (Fig. 3D). GSEA further revealed that low SLC1A6 expression was associated with immune activation pathways (Fig. 3E, F). We then applied the CIBERSORT, ESTIMATE, and ssGSEA algorithms to assess immune infiltration in both groups (Fig. 3G, H). The results showed that the SLC1A6-low group exhibited higher immune infiltration scores and ESTIMATE scores, suggesting enhanced immune infiltration and reduced tumor purity. Furthermore, the SLC1A6-low group exhibited increased infiltration of immune cells, particularly those with antitumor activity, such as T cells (including helper and cytotoxic T cells) and natural killer (NK) cells. We further validated our findings using transcriptomic data from bladder cancer patients in our institution. Consistent with previous analyses, the SLC1A6-high group exhibited downregulation of immune activation-related pathways (Fig. S4A-B). Additionally, pathway enrichment analysis revealed a significant association between high SLC1A6 expression and glutamate metabolism-related pathways, suggesting a potential link between SLC1A6 and glutamate metabolism. Furthermore, no significant differences in SLC1A6 expression were observed across different molecular pathological subtypes (Fig. S4C). We further validated the clinical relevance of SLC1A6 in lung cancer samples from the TCGA database, recapitulating consistent observations (Fig. S4D-F).

Collectively, these findings suggest that SLC1A6 is associated with tumor progression and the formation of an immunosuppressive tumor microenvironment.

## SLC1A6 of tumor cells competitively uptake glutamate to reduce the effector function of $CD8^+$ T cells

Building on our previous analyses, we employed an in vitro co-culture model to validate the impact of SLC1A6 expression in tumor cells on T cell effector function. First, we knocked down SLC1A6 in the mouse bladder cancer cell line MB49. RT-qPCR results confirmed a significant reduction in SLC1A6 mRNA levels in $MB49^{shSLC1A6}$ cells compared to $MB49^{shNC}$ cells (Fig. S5A). Western blot analysis further corroborated the downregulation of SLC1A6 protein expression in $MB49^{shSLC1A6}$ cells (Fig. S5B). Knockdown of SLC1A6 slowed the growth rate of MB49 cells, while the addition of glutamate to the control group $MB49^{shNC}$ cells enhanced their growth ability (Fig. S5C). Similarly, SLC1A6 knockdown reduced the migration ability of MB49 cells, whereas the addition of glutamate enhanced their migration potential (Fig. S5D). Consistent experimental paradigms were applied in murine Lewis lung carcinoma (LLC) cells. Glutamate supplementation enhanced cellular proliferation and migration capacities, whereas SLC1A6 knockdown significantly attenuated these oncogenic phenotypes (Fig. S5E-H).

Next, we measured glutamate levels in $MB49^{shNC}$ and $MB49^{shSLC1A6}$ cells and their culture supernatants. Glutamate content in $MB49^{shSLC1A6}$ cells was decreased, while the glutamate level in the supernatant was increased (Fig. 4A, B). These results suggest that tumor cell SLC1A6 enhances the growth and migration abilities of tumor cells by facilitating the uptake of exogenous glutamate. We speculated whether glutamate might influence the effector function of T cells. Flow cytometry analysis showed that the addition of exogenous glutamate increased the proportion of $GZMB^+CD8^+$ T cells (Fig. 4C, D). Next, we separately added the conditioned medium from $MB49^{shNC}$ and $MB49^{shSLC1A6}$ cells to primary mouse T cells. Flow cytometry analysis revealed a higher proportion of $GZMB^+CD8^+$ T cells in the $MB49^{shSLC1A6}$ group compared to the $MB49^{shNC}$ group. Moreover, the addition of glutamate to the $MB49^{shNC}$ conditioned medium increased the proportion of $GZMB^+CD8^+$ T cells (Fig. 4E, F). The above results suggest that tumor cell SLC1A6 reduces the effector function of $CD8^+$ T cells by competitively taking up glutamate, while both exogenous glutamate supplementation and reduced expression of SLC1A6 in tumor cells enhance the effector function of $CD8^+$ T cells.

## Knockdown of SLC1A6 in MB49 cells enhances the efficacy of anti-PD-1 immunotherapy

To investigate the impact of SLC1A6 knockdown on anti-PD-1 immunotherapy, we established a subcutaneous tumor model with MB49 cells. Mice were injected with $MB49^{shNC}$ or $MB49^{shSLC1A6}$ cells, followed by treatment with anti-PD-1 antibodies or IgG as a control (Fig. 5A). Our results demonstrated that SLC1A6 knockdown inhibited tumor growth to some extent. While anti-PD-1 therapy alone exhibited partial therapeutic efficacy in the MB49 tumor model, the combination of SLC1A6 knockdown and anti-PD-1 treatment significantly enhanced tumor suppression

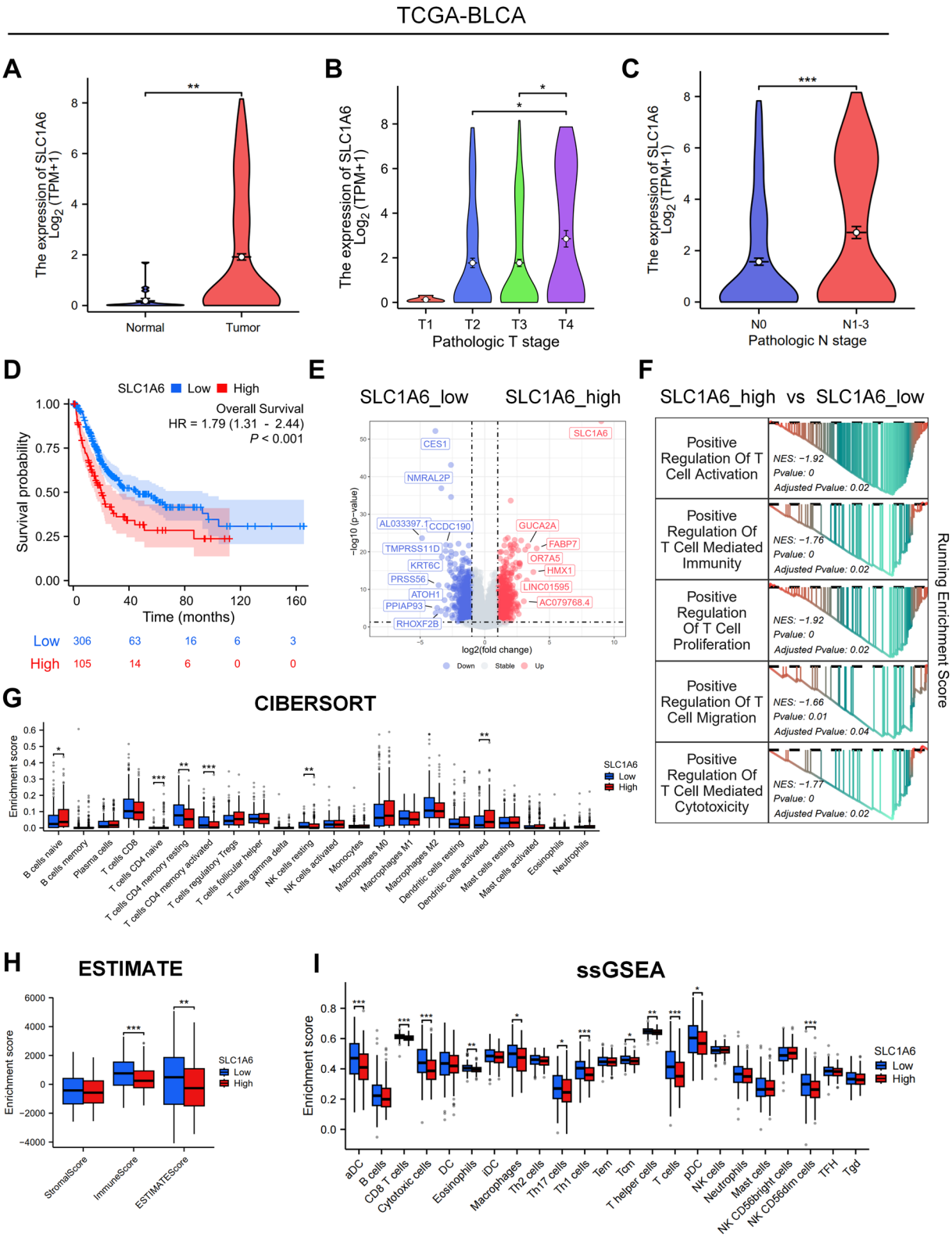


(Fig. 5B–D). Furthermore, immunofluorescence analysis revealed higher infiltration of GZMB$^{+}$CD8$^{+}$ T cells in tumors of the MB49$^{shSLC1A6}$ group receiving anti-PD-1 treatment (Fig. 5E, F). These findings suggest that SLC1A6 knockdown significantly augments the therapeutic efficacy of anti-PD-1 immunotherapy in bladder cancer. To further confirm the role of SLC1A6 knockdown in enhancing immunotherapy efficacy, we also validated this finding

◂**Fig. 3** Correlation of SLC1A6 expression with bladder cancer progression and immune infiltration. **A** Violin plot showing the differential expression of SLC1A6 between bladder cancer and normal tissues from the TCGA database. **B,C** Violin plots showing SLC1A6 expression across different pathological T (**B**) and N (**C**) stages in bladder cancer patients from the TCGA database. **D** Overall survival curve of bladder cancer patients in the SLC1A6-low and SLC1A6-high expression groups from the TCGA database. **E** Volcano plot of differentially expressed genes enriched in the SLC1A6-low and SLC1A6-high groups in bladder cancer samples from the TCGA database. **F** GSEA results illustrating the enriched pathways between the SLC1A6-low and SLC1A6-high groups from the TCGA database. **G** CIBERSORT immune cell composition scores of the SLC1A6-low and SLC1A6-high expression groups in bladder cancer patients from the TCGA database. **H** ESTIMATE scores comparing the SLC1A6-low and SLC1A6-high groups in bladder cancer patients from the TCGA database. **I** ssGSEA-derived immune infiltration scores for the SLC1A6-low and SLC1A6-high groups in bladder cancer patients from the TCGA database

in LLC murine models (Fig. S6A). SLC1A6 knockdown significantly enhanced the therapeutic efficacy of anti-PD-L1, as evidenced by attenuated tumor growth and reduced tumor mass (Fig. S6B-D). In conclusion, targeted SLC1A6 suppression synergistically potentiates immune checkpoint inhibition, as evidenced by improved therapeutic response metrics.

## Discussions

In recent years, ICIs have achieved remarkable breakthroughs in cancer treatment, offering durable survival benefits for patients with advanced disease [23, 24]. As a crucial therapeutic approach, neoadjuvant therapy aims to control tumors prior to surgery via systemic treatment, thereby reducing postoperative recurrence and metastasis while improving overall survival (OS) and disease-free survival (DFS) [25, 26]. The advent of novel ICIs, including nivolumab, atezolizumab, pembrolizumab, and avelumab, has significantly expanded treatment options, offering renewed hope for patients with advanced bladder cancer [27–29]. However, despite these advancements, tumor heterogeneity and acquired resistance to ICIs remain formidable challenges that limit therapeutic efficacy. Addressing these challenges requires a deeper understanding of bladder cancer heterogeneity and the development of precision-based combination strategies tailored to individual patient profiles [30–33]. Therefore, elucidating the molecular mechanisms underlying immunotherapy resistance is paramount for the advancement of more effective therapeutic approaches [34].

Beyond its classical role as a neurotransmitter in the central nervous system, glutamate has emerged as a pivotal regulator of immune responses and tumor immunotherapy [35, 36]. Within the TME, glutamate exerts its influence through high-affinity transporters of the SLC1A family, including SLC1A1, SLC1A2, SLC1A3, SLC1A6, and SLC1A7, as well as through N-methyl-D-aspartate (NMDA) receptors, α-amino-3-hydroxy-5-methyl-4-isoxazolepropionic acid (AMPA) receptors, and metabotropic glutamate receptors (mGluRs) [13, 19]. Moreover, glutamate-mediated metabolic reprogramming plays a crucial role in modulating T cell activation, migration, cytokine secretion, and immune surveillance by altering intracellular calcium homeostasis and cellular metabolism [37, 38]. Previous studies have demonstrated that glutamate-derived metabolites γ-aminobutyric acid (GABA) secreted by B cells can promote the differentiation of monocytes into anti-inflammatory macrophages, thereby attenuating cytotoxic T cell responses and facilitating tumor immune evasion [39, 40]. Beyond glutamate metabolism, other metabolic pathways, such as tryptophan-kynurenine metabolism and lipid metabolism, have also been implicated in immune evasion by suppressing T cell activity and promoting an immunosuppressive TME [41, 42]. Notably, the kynurenine pathway exerts its effects by engaging aryl hydrocarbon receptor (AhR) signaling, while lipid metabolic reprogramming facilitates the accumulation of immunosuppressive macrophages and regulatory T cells [42, 43]. Although therapeutic agents targeting glutamate metabolism, its transporters, and associated signaling pathways have been developed, their clinical efficacy in cancer patients remains to be fully elucidated [13]. As our understanding of glutamate signaling and its interaction with tumor cells and $CD8^+$ T cells continues to advance, targeted modulation of glutamate metabolism may provide novel strategies to enhance tumor immunotherapy and improve patient outcomes.

In this study, we identified the glutamate transporter SLC1A6 as a key mediator of immunotherapy resistance in bladder cancer using single-cell RNA sequencing analysis. The clinical significance of SLC1A6 was further validated using lung cancer single-cell datasets, as well as transcriptomic data from both bladder and lung cancer cohorts, followed by in vitro and in vivo functional assays, confirming its role in promoting resistance to neoadjuvant immunotherapy in cancer. Although previous studies have implicated SLC1A6 in various malignancies, its precise functional contributions remain poorly understood [16–18, 44]. The glutamate metabolic pathways mediated by SLC1A6 in tumor cells are highly intricate and may involve GABA synthesis, glutamine production, and TCA cycle regulation. These metabolic intermediates can directly influence tumor cell physiology or be secreted into the TME, where they modulate $CD8^+$ T cell function and contribute to immune resistance [20, 45, 46]. Building on this, therapeutic strategies targeting SLC1A6 expression or function may restore immune cell activity, enhance tumor antigen recognition, and improve antitumor immune responses. Notably, a study on low-grade gliomas

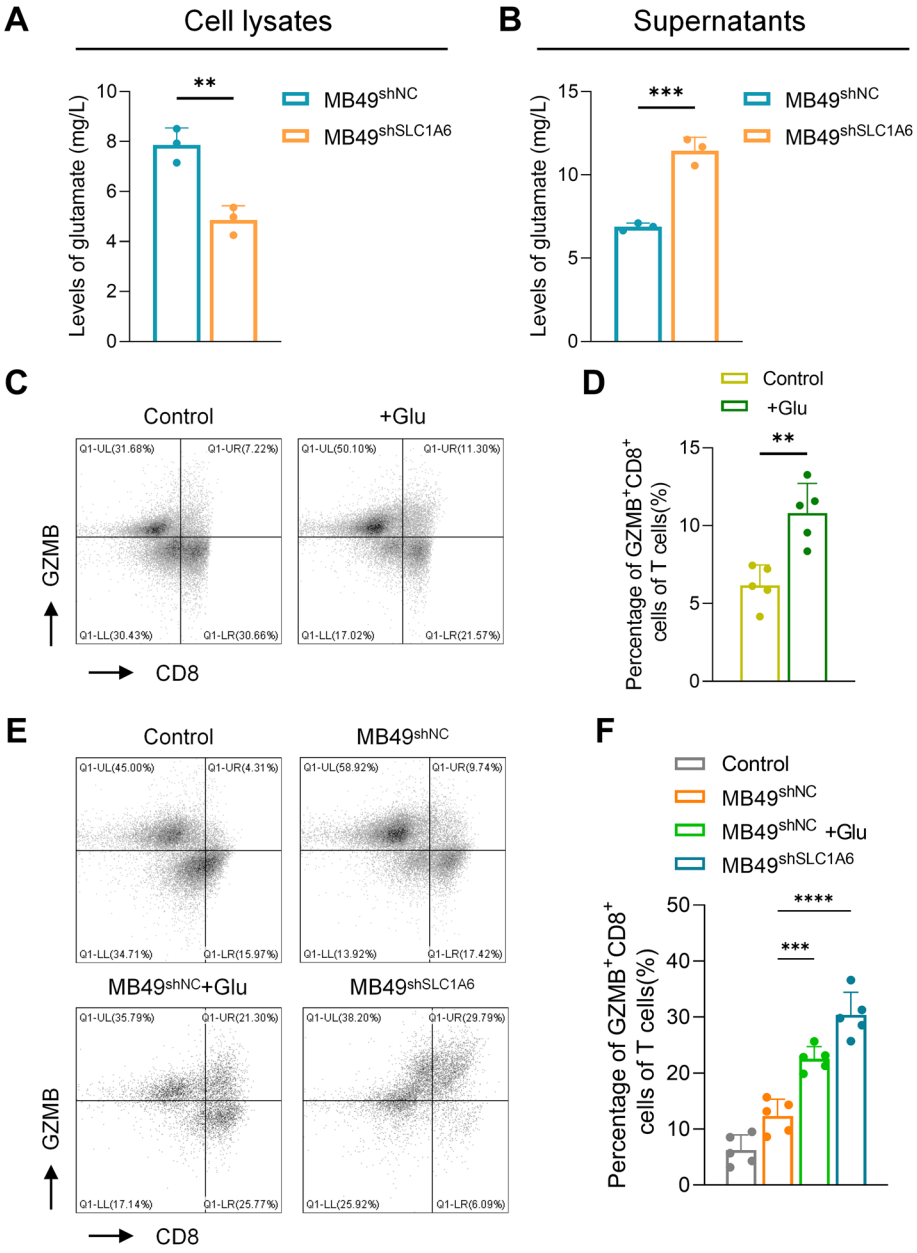


**Fig. 4** Knockdown of SLC1A6 in MB49 cells enhances $CD8^+$ T cells effector function. **A** The glutamate levels in the lysates of $MB49^{shNC}$ and $MB49^{shSLC1A6}$ cells. **B** The glutamate levels in the culture supernatant of $MB49^{shNC}$ and $MB49^{shSLC1A6}$ cells. **C** Flow cytometry representative image showing the effect of exogenous glutamate on mouse primary T cells. **D** Flow cytometry statistical analysis showing the effect of exogenous glutamate on mouse primary T cells. **E** Flow cytometry representative image showing the effect of conditioned medium from $MB49^{shNC}$ and $MB49^{shSLC1A6}$ cells on mouse primary T cells. **F** Flow cytometry statistical analysis showing the effect of conditioned medium from $MB49^{shNC}$ and $MB49^{shSLC1A6}$ cells on mouse primary T cells. Glu: glutamate

reported that reduced SLC1A6 expression was associated with increased immune cell infiltration and heightened sensitivity to immune checkpoint blockade therapy [47], which aligns with our observations. Furthermore, research on nasopharyngeal carcinoma has demonstrated that radioresistant tumor cells exhibit diminished sensitivity to chemotherapy, potentially due to increased SLC1A6 expression, which upregulates drug resistance genes and reduces cisplatin sensitivity [44]. Zou et al. [17] identified SLC1A6 as an independent prognostic factor for poor outcomes in bladder cancer, a conclusion further supported by Wang et al. [48], who reported that elevated SLC1A6 expression correlates with a higher risk of muscle-invasive bladder cancer and shorter survival.

Despite the significant clinical implications of SLC1A6 in cancer immunotherapy, this study has several limitations. First, the current findings are primarily derived from bladder cancer and partially validated in lung cancer, limiting the generalizability of our conclusions across other tumor types. Future studies involving a broader spectrum of cancers are necessary to determine whether the immunoregulatory role of SLC1A6 is conserved across malignancies. Additionally, the precise mechanisms by which SLC1A6 and glutamate metabolism regulate $CD8^+$ T cell function remain to be fully elucidated. Future research should focus on identifying the key molecular pathways and biological processes that govern SLC1A6-mediated immune evasion and immunotherapy resistance. Finally,

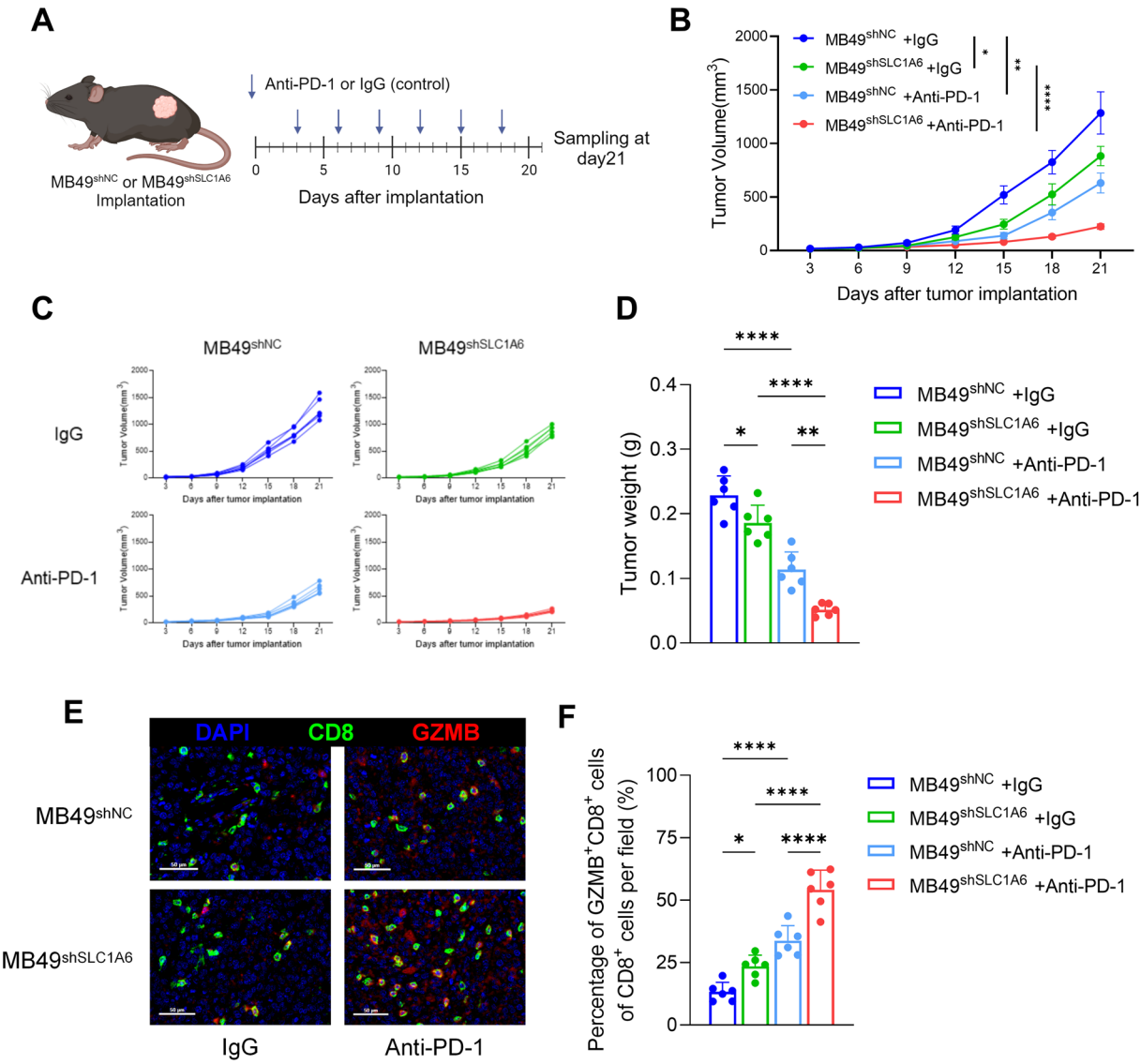


**Fig. 5** Knockdown of SLC1A6 in MB49 cells enhances the efficacy of anti-PD-1 immunotherapy. **A** Overview of the experimental design, where mice with subcutaneous tumors derived from $MB49^{shNC}$ or $MB49^{shSLC1A6}$ cells were assigned to two treatment groups, receiving either IgG control or anti-PD-1 therapy. **B** Tumor growth curves of the four groups over the 21-day experimental period. **C** Group-specific tumor growth curves of the four groups over the 21-day experimental period. **D** Tumor weight statistics from four groups of mice at day 21. **E** Representative immunofluorescence images illustrating the infiltration of $GZMB^+CD8^+$ T cells in tumor samples from the four groups. **F** Statistical analysis of the proportion of $GZMB^+CD8^+$ T cells detected by immunofluorescence across the groups

in the context of precision oncology, continued efforts should focus on developing and systematically evaluating therapeutic strategies targeting SLC1A6, with particular attention to their efficacy and safety in diverse, real-world clinical settings.

In conclusion, our study identifies SLC1A6 as a novel biomarker and potential therapeutic target in cancer, providing valuable insights into its prognostic significance. Targeting SLC1A6 may offer a promising strategy to overcome resistance to neoadjuvant immunotherapy and facilitate the development of combination treatment approaches, ultimately improving therapeutic outcomes in cancer.

**Supplementary Information** The online version contains supplementary material available at https://doi.org/10.1007/s00262-025-04074-4.

**Acknowledgements** The single-cell RNA sequencing was performed in Shanghai Biotechnology Co., Ltd. (Shanghai, China).

**Author contributions** Chenchen Li contributed to investigation, methodology, formal analysis, software, visualization, writing—reviewing and editing, and supervision. Yi Lin and Haoran Zheng contributed to

investigation, methodology, formal analysis, software, visualization, and writing—original draft. Hengda Zeng contributed to investigation, methodology, formal analysis, writing—reviewing and editing, and supervision. Longhao Xu contributed to investigation, formal analysis, software, and visualization. Daqin Wu performed investigation, formal analysis, and supervision. Jianwen Lao and Shuai Liang contributed to resources and data curation. Peicong Cai contributed to resources and writing—reviewing and editing. Chunhui Wang was involved in funding acquisition. Tianxin Lin and Wenlong Zhong contributed to conceptualization, supervision, and funding acquisition.

**Funding** This research was funded by National Natural Science Foundation of China (Grant No. 82373254 and 82260503), Guangdong Provincial Natural Science Foundation (Grant No. 2023A1515010258), Sun Yat-Sen Memorial Hospital Clinical Research 5010 Program (Grant No. SYS-5010Z-202401), Science and Technology Talent and Platform Program (Yunnan Academician and Expert Workstation) (202305AF150136), and Yunnan Provincial Department of Science and Technology Program (Basic Research Special Fund) (202301AS070077).

**Data availability** The data used to support the findings of this study are available from the corresponding author upon request.

## Declarations

**Conflict of interest** The authors declare no competing interests.

**Consent for publication** All the authors approved the publication of the manuscript.

**Ethical approval** The study was approved by the Ethics Committees of Sun Yat-Sen Memorial Hospital, Sun Yat-Sen University (SYSKY-2024-1158-01). For animal study, the procedures for care and use of animals were approved by the Ethics Committee of the TopbiotechBiotechnology Co., Ltd (LFTOP-IACUC-2025-0003).



## References

1. Flaig TW, Spiess PE, Abern M, Agarwal N, Bangs R, Buyyounouski MK et al (2024) NCCN guidelines(R) insights: bladder cancer, version 3.2024. J Natl Compr Cancer Netw. 22(4):216–225
2. Bamias A, Davis ID, Galsky MD, Arranz JA, Kikuchi E, Grande E et al (2024) Atezolizumab monotherapy versus chemotherapy in untreated locally advanced or metastatic urothelial carcinoma (IMvigor130): final overall survival analysis from a randomised, controlled, phase 3 study. Lancet Oncol 25(1):46–61
3. Patel VG, Oh WK, Galsky MD (2020) Treatment of muscle-invasive and advanced bladder cancer in 2020. CA Cancer J Clin 70(5):404–423
4. Lawrence MS, Stojanov P, Polak P, Kryukov GV, Cibulskis K, Sivachenko A et al (2013) Mutational heterogeneity in cancer and the search for new cancer-associated genes. Nature 499(7457):214–218
5. Grivennikov SI, Greten FR, Karin M (2010) Immunity, inflammation, and cancer. Cell 140(6):883–899
6. Schneider AK, Chevalier MF, Derre L (2019) The multifaceted immune regulation of bladder cancer. Nat Rev Urol 16(10):613–630
7. Joseph M, Enting D (2019) Immune responses in bladder cancer-role of immune cell populations, prognostic factors and therapeutic implications. Front Oncol 9:1270
8. Gonzalez H, Hagerling C, Werb Z (2018) Roles of the immune system in cancer: from tumor initiation to metastatic progression. Genes Dev 32(19–20):1267–1284
9. Balar AV, Galsky MD, Rosenberg JE, Powles T, Petrylak DP, Bellmunt J et al (2017) Atezolizumab as first-line treatment in cisplatin-ineligible patients with locally advanced and metastatic urothelial carcinoma: a single-arm, multicentre, phase 2 trial. Lancet 389(10064):67–76
10. Hoffman-Censits J, Pal S, Kaiser C, Ding B, Bellmunt J (2020) Atezolizumab in patients with renal insufficiency and mixed variant histology: analyses from an expanded access program in platinum-treated locally advanced or metastatic urothelial carcinoma. J Immunother Cancer 8(2):e000419
11. Bruni D, Angell HK, Galon J (2020) The immune contexture and Immunoscore in cancer prognosis and therapeutic efficacy. Nat Rev Cancer 20(11):662–680
12. Knowles MA, Hurst CD (2015) Molecular biology of bladder cancer: new insights into pathogenesis and clinical diversity. Nat Rev Cancer 15(1):25–41
13. Kanai Y, Clemencon B, Simonin A, Leuenberger M, Lochner M, Weisstanner M et al (2013) The SLC1 high-affinity glutamate and neutral amino acid transporter family. Mol Aspects Med 34(2–3):108–120
14. Zhou Y, Danbolt NC (2013) GABA and glutamate transporters in brain. Front Endocrinol (Lausanne) 4:165
15. Magi S, Piccirillo S, Amoroso S, Lariccia V (2019) Excitatory amino acid transporters (EAATs): glutamate transport and beyond. Int J Mol Sci 20(22):5674
16. Kumar K, Banerjee Dixit A, Tripathi M, Dubey V, Siraj F, Sharma MC et al (2022) Transcriptomic profiling of nonneoplastic cortical tissues reveals epileptogenic mechanisms in dysembryoplastic neuroepithelial tumors. Funct Integr Genomics 22(5):905–917
17. Zou X, Wei Y, Qi T, Wang X, Zuo W, Wang T et al (2021) A novel 6-gene signature derived from tumor-infiltrating T cells and neutrophils predicts survival of bladder urothelial carcinoma. Aging (Albany NY) 13(23):25496–25517
18. Yue Y, Deng P, Xiao H, Tan M, Wang H, Tian L et al (2022) N6-methyladenosine-mediated downregulation of miR-374c-5p promotes cadmium-induced cell proliferation and metastasis by targeting GRM3 in breast cancer cells. Ecotoxicol Environ Saf 229:113085
19. Koda S, Hu J, Ju X, Sun G, Shao S, Tang RX et al (2023) The role of glutamate receptors in the regulation of the tumor microenvironment. Front Immunol 14:1123841
20. Olsen GM, Sonnewald U (2015) Glutamate: where does it come from and where does it go? Neurochem Int 88:47–52
21. Anderson NM, Mucka P, Kern JG, Feng H (2018) The emerging role and targetability of the TCA cycle in cancer metabolism. Protein Cell 9(2):216–237

22. Park SJ, Yoo HC, Ahn E, Luo E, Kim Y, Sung Y et al (2023) Enhanced glutaminolysis drives hypoxia-induced chemoresistance in pancreatic cancer. Cancer Res 83(5):735–752
23. Bilim V, Kuroki H, Shirono Y, Murata M, Hiruma K, Tomita Y (2022) Advanced bladder cancer: changing the treatment landscape. J Pers Med 12(10):1745
24. Hu J, Chen J, Ou Z, Chen H, Liu Z, Chen M et al (2022) Neoadjuvant immunotherapy, chemotherapy, and combination therapy in muscle-invasive bladder cancer: a multi-center real-world retrospective study. Cell Rep Med 3(11):100785
25. Topalian SL, Taube JM, Pardoll DM (2020) Neoadjuvant checkpoint blockade for cancer immunotherapy. Science 367(6477):eaax0182
26. Topalian SL, Forde PM, Emens LA, Yarchoan M, Smith KN, Pardoll DM (2023) Neoadjuvant immune checkpoint blockade: a window of opportunity to advance cancer immunotherapy. Cancer Cell 41(9):1551–1566
27. van Dijk N, Gil-Jimenez A, Silina K, Hendricksen K, Smit LA, de Feijter JM et al (2020) Preoperative ipilimumab plus nivolumab in locoregionally advanced urothelial cancer: the NABUCCO trial. Nat Med 26(12):1839–1844
28. Bellmunt J, Hussain M, Gschwend JE, Albers P, Oudard S, Castellano D et al (2021) Adjuvant atezolizumab versus observation in muscle-invasive urothelial carcinoma (IMvigor010): a multicentre, open-label, randomised, phase 3 trial. Lancet Oncol 22(4):525–537
29. Burtness B, Harrington KJ, Greil R, Soulieres D, Tahara M, de Castro G Jr et al (2019) Pembrolizumab alone or with chemotherapy versus cetuximab with chemotherapy for recurrent or metastatic squamous cell carcinoma of the head and neck (KEYNOTE-048): a randomised, open-label, phase 3 study. Lancet 394(10212):1915–1928
30. Lobo N, Martini A, Kamat AM (2022) Evolution of immunotherapy in the treatment of non-muscle-invasive bladder cancer. Expert Rev Anticancer Ther 22(4):361–370
31. Sharma P, Callahan MK, Bono P, Kim J, Spiliopoulou P, Calvo E et al (2016) Nivolumab monotherapy in recurrent metastatic urothelial carcinoma (CheckMate 032): a multicentre, open-label, two-stage, multi-arm, phase 1/2 trial. Lancet Oncol 17(11):1590–1598
32. Wu Z, Liu J, Dai R, Wu S (2021) Current status and future perspectives of immunotherapy in bladder cancer treatment. Sci China Life Sci 64(4):512–533
33. Hegde PS, Chen DS (2020) Top 10 Challenges in Cancer Immunotherapy. Immunity 52(1):17–35
34. Rey-Cardenas M, Guerrero-Ramos F, Gomez de Liano Lista A, Carretero-Gonzalez A, Bote H, Herrera-Juarez M et al (2021) Recent advances in neoadjuvant immunotherapy for urothelial bladder cancer: What to expect in the near future. Cancer Treat Rev 93:102142
35. Rzeski W, Ikonomidou C, Turski L (2002) Glutamate antagonists limit tumor growth. Biochem Pharmacol 64(8):1195–1200
36. Kelly B, Pearce EL (2020) Amino assets: how amino acids support immunity. Cell Metab 32(2):154–175
37. Pacheco R, Gallart T, Lluis C, Franco R (2007) Role of glutamate on T-cell mediated immunity. J Neuroimmunol 185(1–2):9–19
38. Pacheco R, Oliva H, Martinez-Navio JM, Climent N, Ciruela F, Gatell JM et al (2006) Glutamate released by dendritic cells as a novel modulator of T cell activation. J Immunol 177(10):6695–6704
39. Zhang B, Vogelzang A, Miyajima M, Sugiura Y, Wu Y, Chamoto K et al (2021) B cell-derived GABA elicits IL-10(+) macrophages to limit anti-tumour immunity. Nature 599(7885):471–476
40. Shi Y (2022) Linking B cell metabolism to immune regulation: the neurotransmitter GABA. Signal Transduct Target Ther 7(1):260
41. Seo SK, Kwon B (2023) Immune regulation through tryptophan metabolism. Exp Mol Med 55(7):1371–1379
42. Martin-Perez M, Urdiroz-Urricelqui U, Bigas C, Benitah SA (2022) The role of lipids in cancer progression and metastasis. Cell Metab 34(11):1675–1699
43. Campesato LF, Budhu S, Tchaicha J, Weng CH, Gigoux M, Cohen IJ et al (2020) Blockade of the AHR restricts a Treg-macrophage suppressive axis induced by L-Kynurenine. Nat Commun 11(1):4011
44. Hao W, Wu L, Cao L, Yu J, Ning L, Wang J et al (2021) Radioresistant nasopharyngeal carcinoma cells exhibited decreased cisplatin sensitivity by inducing SLC1A6 expression. Front Pharmacol 12:629264
45. Walker MC, van der Donk WA (2016) The many roles of glutamate in metabolism. J Ind Microbiol Biotechnol 43(2–3):419–430
46. Rowley NM, Madsen KK, Schousboe A, Steve WH (2012) Glutamate and GABA synthesis, release, transport and metabolism as targets for seizure control. Neurochem Int 61(4):546–558
47. Li J, Guo Q, Xing R (2023) Construction and validation of an immune infiltration-related risk model for predicting prognosis and immunotherapy response in low grade glioma. BMC Cancer 23(1):727
48. Wang H, Dai Y, Wu X, Hu B, Wang Z, Yan M (2022) Multi-omics analysis of ferroptosis-related molecular subtypes in muscle-invasive bladder cancer immunotherapy. Transl Cancer Res 11(11):4089–4104